

Adaptive liquid lens actuated by liquid crystal pistons

Su Xu,¹ Hongwen Ren,² and Shin-Tson Wu^{1,*}

¹CREOL, The College of Optics and Photonics, University of Central Florida, Orlando, Florida 32816, USA
²Department of Polymer Nano-Science and Engineering, Chonbuk National University, Chonju, Chonbuk 561-756, South Korea

*swu@mail.ucf.edu

Abstract: An adaptive liquid lens actuated by liquid crystal (LC) pistons is demonstrated. It adopts fluid pressure introduced by the reciprocating movement of LC droplets to regulate the liquid-air interface which, in turn, changes the optical power of the resultant liquid lens. The competitive features are compact size, simple fabrication, good optical performance, reasonably fast response time and low power consumption. Since the actuation power can be enhanced by increasing the number of LC pistons rather than the operating voltages, it is possible to significantly actuate a large-aperture lens or lens array at a relatively low operating voltage.

©2012 Optical Society of America

OCIS codes: (010.1080) Active or adaptive optics; (220.3620) Lens system design; (160.3710) Liquid crystals; (230.2090) Electro-optical devices.

References

1. N. Sugiura and S. Morita, "Variable-focus liquid-filled optical lens," *Appl. Opt.* **32**(22), 4181–4186 (1993).
2. H. Oku and M. Ishikawa, "High-speed liquid lens with 2 ms response and 80.3 nm root-mean-square wavefront error," *Appl. Phys. Lett.* **94**(22), 221108 (2009).
3. H. Ren, D. Fox, P. A. Anderson, B. Wu, and S.-T. Wu, "Tunable-focus liquid lens controlled using a servo motor," *Opt. Express* **14**(18), 8031–8036 (2006).
4. C.-S. Liu and P. D. Lin, "Miniaturized auto-focusing VCM actuator with zero holding current," *Opt. Express* **17**(12), 9754–9763 (2009).
5. H.-M. Son, M. Y. Kim, and Y.-J. Lee, "Tunable-focus liquid lens system controlled by antagonistic winding-type SMA actuator," *Opt. Express* **17**(16), 14339–14350 (2009).
6. A. Pouydebasque, C. Bridoux, F. Jacquet, S. Moreau, E. Sage, D. Saint-Patrice, C. Bouvier, C. Kopp, G. Marchand, S. Bolis, N. Sillon, and E. Vigier-Blanc, "Varifocal liquid lenses with integrated actuator, high focusing power and low operating voltage fabricated on 200 mm wafers," *Sens. Actuators A Phys.* **172**(1), 280–286 (2011).
7. W. Zhang, K. Aljaseem, H. Zappe, and A. Seifert, "Completely integrated, thermo-pneumatically tunable microlens," *Opt. Express* **19**(3), 2347–2362 (2011).
8. S. W. Lee and S. S. Lee, "Focal tunable liquid lens integrated with an electromagnetic actuator," *Appl. Phys. Lett.* **90**(12), 121129 (2007).
9. B. A. Malouin, Jr., M. J. Vogel, J. D. Olles, L. Cheng, and A. H. Hirsra, "Electromagnetic liquid pistons for capillarity-based pumping," *Lab Chip* **11**(3), 393–397 (2011).
10. H.-C. Cheng, S. Xu, Y. Liu, S. Levi, and S.-T. Wu, "Adaptive mechanical-wetting lens actuated by ferrofluids," *Opt. Commun.* **284**(8), 2118–2121 (2011).
11. W.-S. Seo, K. Yoshida, S. Yokota, and K. Edamura, "A high performance planar pump using electro-conjugate fluid with improved electrode patterns," *Sens. Actuators A Phys.* **134**(2), 606–614 (2007).
12. S. I. Son, D. Pugal, T. Hwang, H. R. Choi, J. C. Koo, Y. Lee, K. Kim, and J.-D. Nam, "Electromechanically driven variable-focus lens based on transparent dielectric elastomer," *Appl. Opt.* **51**(15), 2987–2996 (2012).
13. S. Xu, H. Ren, Y.-J. Lin, M. G. J. Moharam, S.-T. Wu, and N. Tabiryan, "Adaptive liquid lens actuated by photo-polymer," *Opt. Express* **17**(20), 17590–17595 (2009).
14. C. A. López, C.-C. Lee, and A. H. Hirsra, "Electrochemically activated adaptive liquid lens," *Appl. Phys. Lett.* **87**(13), 134102 (2005).
15. L. Miccio, A. Finizio, S. Grilli, V. Vespini, M. Paturzo, S. De Nicola, and P. Ferraro, "Tunable liquid microlens arrays in electrode-less configuration and their accurate characterization by interference microscopy," *Opt. Express* **17**(4), 2487–2499 (2009).
16. L. Dong, A. K. Agarwal, D. J. Beebe, and H. Jiang, "Adaptive liquid microlenses activated by stimuli-responsive hydrogels," *Nature* **442**(7102), 551–554 (2006).

17. M. Vallet, B. Berge, and L. Vovelle, "Electrowetting of water and aqueous solutions on poly(ethylene terephthalate) insulating films," *Polymer* **37**(12), 2465–2470 (1996).
18. C.-C. Cheng and J. A. Yeh, "Dielectrically actuated liquid lens," *Opt. Express* **15**(12), 7140–7145 (2007).
19. H. Ren, S. Xu, and S.-T. Wu, "Voltage-expandable liquid crystal surface," *Lab Chip* **11**(20), 3426–3430 (2011).
20. P. Penfield and H. A. Haus, "*Electrodynamics of moving media*", (MIT, 1967).
21. S. Xu, H. Ren, Y. Liu, and S. T. Wu, "Color displays based on voltage-stretchable liquid crystal droplet," *J. Disp. Technol.* **8**(6), 336–340 (2012).
22. D. Zhu, C. Li, X. Zeng, and H. Jiang, "Tunable-focus microlens arrays on curved surfaces," *Appl. Phys. Lett.* **96**(8), 081111–081113 (2010).
23. H. Ren, S. Xu, and S. T. Wu, "Liquid crystal pump," *Lab Chip* **13**(1), 100–105 (2013).
24. S. Xu, Y. Liu, H. Ren, and S.-T. Wu, "A novel adaptive mechanical-wetting lens for visible and near infrared imaging," *Opt. Express* **18**(12), 12430–12435 (2010).
25. H. Ren, S. Xu, and S.-T. Wu, "Effects of gravity on the shape of liquid droplets," *Opt. Commun.* **283**(17), 3255–3258 (2010).

1. Introduction

Adaptive liquid lenses, which are based on physical adjustment of the lens shape, have the advantages of intrinsic smooth interface, adaptively tuned or reconfigured output, polarization insensitive, broadband, and vibration resistance if two density-matched liquids are employed. Promising applications include cellphone cameras, image processing, optical communication, sensors and vision devices. Various operating principles have been proposed: fluidic pressure [1–13], electrochemistry [14], thermal effect [15], environmentally adaptive hydrogel [16], electro-wetting [17], and dielectrophoresis [18]. Among them, fluidic pressure is the most straightforward way to dynamically manipulate the optical interface formed by liquids. The fluidic pressure can be provided by external pumps [1], mechanical systems (e.g. piezoelectric actuator [2], servo motor [3], voice coil motor [4] and shape memory alloy [5], electrostatic actuator [6], thermal actuator [7], electromagnetic actuator [8], ferrofluids [9, 10], electro-conjugate fluids [11], artificial muscle [12], and photo-polymer [13], etc. Compared to other operating principles, it is possible to actuate a large-aperture lens and significantly tune the liquid-air (or liquid-liquid) interface by fluidic pressure [1–5]. However, there are some technical challenges: bulky size [1–5], performance degradation [1–5], limited stable working range [6], slow response time [7], large power consumption [8–10], high operating voltage [11, 12] and weak actuation power [11–13].

In this paper, we demonstrate an adaptive liquid lens actuated by LC pistons. The lens cell consists of a top acrylic slab drilled with an aperture hole and several reservoir holes, and a bottom glass slab with interdigitated indium tin oxide (ITO) electrodes. In each reservoir hole, a small volume of LC forms a pillar-like droplet and touches the bottom slab. The surrounding liquid forms a lens shape at the aperture hole. As the voltage increases, the LC in contact with the bottom substrate is stretched by the dielectric force and an extra volume of LC is pulled into the lens chamber through the reservoir holes. The exerted fluidic pressure leads to a change in the lens profile and the corresponding optical power. Upon removing the voltage, the LC droplet returns to the original state and the lens also recovers. The LC droplet with such a reciprocating movement functions like a piston and can effectively tune the optical power of the liquid lens. This actuation method works for lens and lens array with aperture size varying from micrometers to centimeters. Compared with other fluidic pressure-actuated liquid lenses [1–13], our lens has the competitive advantages in compact size, simple structure, reasonably fast response time and low power consumption. Furthermore, since the actuation power can be enhanced by increasing the number of LC pistons rather than the operating voltages, it is possible to significantly actuate a large-aperture lens or lens array at a relatively low operating voltage.

2. Device structure and operation principles

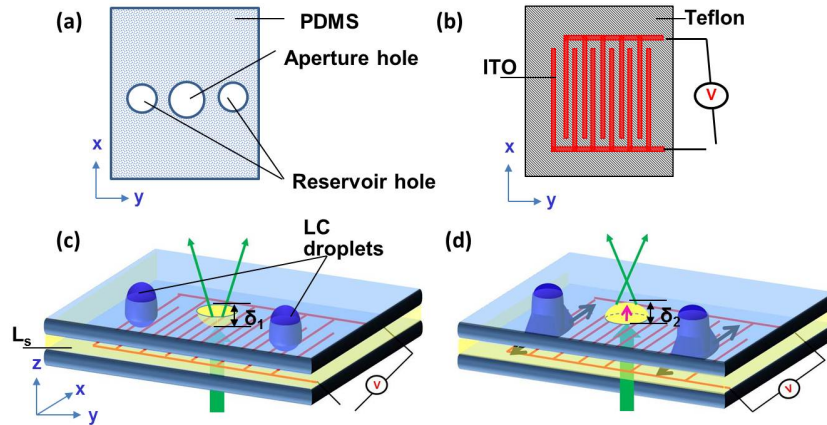


Fig. 1. (a) The layout of lens hole and reservoir holes on the top acrylic slab, (b) the layout of the interdigitated ITO electrode and Teflon layer on the bottom glass slab (the aperture and width of ITO stripes are not drawn by scale.), (c) liquid lens and LC pistons are at rest state, and (d) liquid lens is actuated by LC pistons.

Figure 1 shows the structure of the proposed adaptive liquid lens. The lens cell consists of a top acrylic slab and a bottom glass slab with a certain cell gap, and the periphery of the cell is sealed by glue. One aperture hole and two reservoir holes are drilled on the top slab, both surfaces of the top slab are coated with polydimethylsiloxane (PDMS, Dow Corning, $\gamma_{PDMS} \sim 20$ mN/m, thickness ~ 1 μm), as Fig. 1(a) shows. The detailed layout of bottom substrate is shown in Fig. 1(b). The inner surface of the bottom slab is coated with interdigitated ITO electrodes (marked as red) and a Teflon layer (400S1-100-1, DuPont, $\gamma_T \sim 19$ mN/m, ~ 1 μm thickness, marked as gray) in sequence. It helps to provide a suitable contact angle for the LC droplet on the bottom slab and prevent the carrier injection [19]. A small amount of LC forms a pillar-like droplet in each reservoir hole, which is in contact with the bottom slab. To lower the operating voltage, here we chose Merck nematic LC mixture ZLI-4389 ($\epsilon_{//} = 56$, $\Delta\epsilon = 45.6$, $\gamma \sim 38$ mN/m, $\langle n \rangle \sim 1.58$, $\rho \sim 0.98$ g/cm³) because it has a large dielectric constant and a low surface tension [19]. The surrounding is filled with immiscible liquid (L_s) silicone oil ($\epsilon \sim 2.9$, $\gamma \sim 21$ mN/m, $n \sim 1.4$, $\rho \sim 0.97$ g/cm³), which forms a lens shape on the aperture hole [Fig. 1(c)]. In the voltage-off state, the LC segment exhibits a near-spherical shape on the top slab due to the hydrophobic property of PDMS, and the LC droplet in the chamber has a minimal surface-to-volume ratio. When a voltage is applied to the bottom electrodes, a nonuniform lateral electric field is generated across the ITO stripes and a dielectric force is exerted on the LC- L_s interface [20]. As the voltage increases, the LC molecules at the droplet border near the bottom slab (within the penetration depth of the electric fields) are reoriented by fringing field, leading to a much larger dielectric constant (close to $\epsilon_{//} = 56$) than that of the silicone oil. Therefore, the LC near the bottom slab bears the strongest dielectric force. The force is pointed outwards, but only the horizontal component will deform the LC droplet. If the voltage is sufficiently high, the LC will be stretched outward along the electrodes (x -direction) in order to reach a new balance between the interfacial tension and dielectric force [21]. As a result, an extra volume of LC is pulled into the chamber, which in turn pushes the silicone oil to overflow towards the aperture hole. Because the volumes of liquids (LC and L_s) are not constricting, the redistribution of liquids changes the liquid-air interface at the aperture hole and the optical power of the resultant liquid lens [Fig. 1(d)]. The pressure exerted on silicone oil (at the lens aperture area) and the dielectric forces exerted on LC pistons are illustrated by pink and black arrows, respectively, as shown in Fig. 1(d). Since the LC droplets are stretched along x -direction, there is no crosstalk between the LC pistons and

liquid lens. Upon removing the voltage, the LC droplet will return to its original state because of the interfacial tension, and so does the liquid lens.

3. Experimental results and discussion

To prove concept, we fabricated a liquid lens actuated by four LC pistons, as shown in Fig. 2(a). The diameters of the four reservoir holes and the aperture hole are 1.5 mm and 2 mm, respectively. The thickness of the top slab is 1 mm, and the cell gap is 0.5 mm. The total thickness of the cell is ~ 2.5 mm. The width and gap of the interdigitated ITO electrodes are both $10\ \mu\text{m}$. The image performance of the LC-piston-actuated lens was evaluated through an optical microscope. The cell was horizontally placed on the microscope stage, and a small number “3” was placed under the cell as an object. Figure 2(b) is the image observed through the microscope without the liquid lens. After inserting the liquid lens in the optical path and refocusing the microscope, a virtual erect and diminished image is observed [Fig. 2(c)], which indicates the liquid lens has a negative optical power at $V = 0$. Then the image begins to grow at $\sim 40\ \text{V}_{\text{rms}}$, and keeps growing when the voltage is further increased. It is because more LC is pulled into the lens chamber with the increased voltage, the surface of the liquid lens becomes flatter and the optical power goes less negative (Figs. 2(e)-(g)). Some image aberration is observed at the border, because the aperture hole drilled on the top acrylic slab is not perfectly circular, and the defects in the circumference introduce the image aberration. Here the fluid lens presents a parabolic shape, spherical aberration is reduced, but coma occurs when the object lies off axis and it increases with the object’s offset from optical axis.

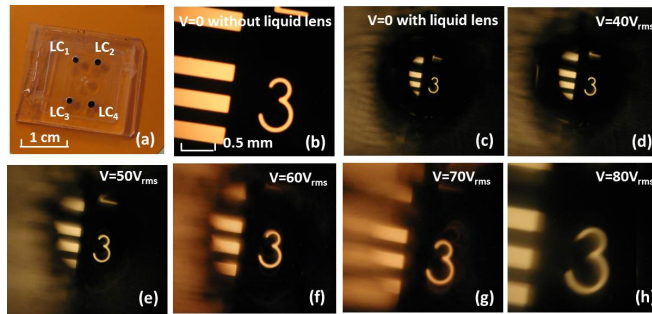


Fig. 2. (a) Lens cell, (b) the images observed through the microscope without the liquid lens at $V = 0$, and (d)-(k) with the liquid lens at the specified voltages (Media 1).

A dynamic switch of the liquid lens between $V = 0$ (in-focus state) and $V = 50\ \text{V}_{\text{rms}}$ (out-of-focus state) is shown in Fig. 2(e) (Media 1). At $V = 80\ \text{V}_{\text{rms}}$, the erected image is magnified, implying the liquid lens exhibits a positive optical power [Fig. 2(h)]. Here the image is a little bit blurry, because it is out of the microscope’s working range. Further increase in the positive optical power is quite limited even when the voltage keeps increasing. A possible explanation is given as follows. Due to our facility limitation, we can only drill holes on the acrylic slab and coat PDMS material as the hydrophobic layers, because acrylic cannot withstand the high baking temperature of Teflon ($\sim 360^\circ\text{C}$). The relative low surface tension of silicone oil ($\gamma \sim 21\ \text{mN/m}$) and PDMS ($\gamma \sim 20\ \text{mN/m}$) cannot effectively confine the liquid-air interface at the aperture hole, and the silicone oil droplet begins to spread on the top substrate when the voltage is further increased. Therefore, to improve the lens’ performance and widen the dynamic range, the top slab is preferred to be a thin glass substrate (or silicon wafer) coated with high quality Teflon layer. The aperture holes should be fabricated in high precision [2] and the inner wall of the hole coated with a hydrophilic layer [22].

Figures 3(a)-(b) show the image properties of the lens and the deformation of LC pistons under white light illumination. For easy observation, we doped $\sim 0.3\ \text{wt}\%$ blue dye (M-137) into the LC mixture. A small bunch of flower was picked as an object. At $V = 0$, the four LC droplets were at rest state, and the object distance was intentionally adjusted to obtain an out-

of-focus (blurred) image [Fig. 3(a)]. At $V = 80V_{\text{rms}}$, the LC droplets were stretched along the electrodes, and the optical power adjustment brought the object into focus, leading to a sharp and clear image [Fig. 3(b)]. The two sub-images in blue circles show the magnified detail of the images taken through the aperture hole, and those in pink squares show a side-view of the LC segments on the top substrate. A top-view deformation of the LC pistons as well as a dynamic transition of the lens (between 0 and $V = 80V_{\text{rms}}$) are recorded as [Media 2](#) and [Media 3](#), respectively, as Fig. 3(b) shows. At the rest state, the lens' resolution is ~ 13 lp/mm [23].

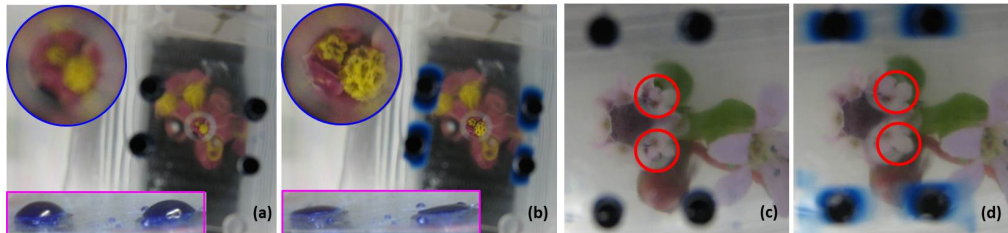


Fig. 3. The images taken through the aperture under white light illumination and the deformation of LC pistons. Single liquid lens actuated by four LC pistons at (a) $V = 0$ and (b) $V = 80V_{\text{rms}}$ ([Media 2](#) and [Media 3](#)), and two liquid lenses actuated by four LC pistons at (c) $V = 0$ and (d) $V = 80V_{\text{rms}}$ ([Media 4](#)).

The back focal distance (BFD) of the liquid lens at various voltages was measured at $\lambda = 633$ nm. The collimated and expanded He-Ne laser beam was normally incident on the lens. Here we intentionally set the exterior surface of the top slab as the last surface of the lens, because it was very difficult to measure the distance (δ_1 and δ_2) between the apex of the liquid-air interface and that exterior surface accurately, as shown in Figs. 1(c)-(d). For the positive lens, the focal point was determined by the smallest focused point of the input beam along the optic axis, while for the negative lens, BFD was determined by a geometrical imaging method [24]. At $V = 0$, the BFD was calculated to be about -5.5 mm. As the voltage increases to $40V_{\text{rms}}$ the BFD firstly goes to negative infinity, and then comes in from positive infinity to ~ 66.5 mm at $V = 80V_{\text{rms}}$, as Fig. 4(a) depicts. Response time was measured by monitoring the time-dependent transmittance change. Here we used a positive solid lens to converge the divergent beam coming from the liquid lens. At $V = 0$, the photodiode detector placed close to the focal point of the two lens system receives the highest intensity. At $70V$ (500Hz) square voltage bursts, the liquid lens becomes less negative and the detected light intensity decreases. From Fig. 4(b), the fall and rise time are ~ 15.2 ms and 19.6 ms, respectively.

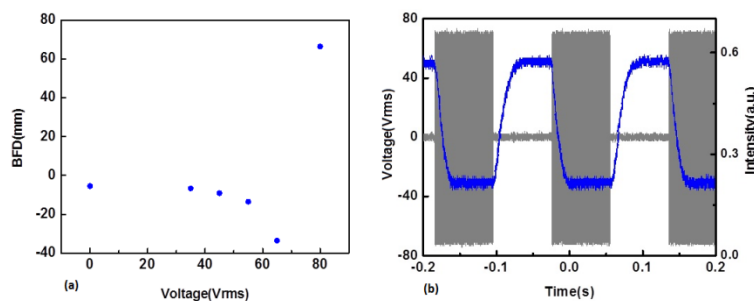


Fig. 4. The measured (a) BFD and (b) response time under 70V square pulses.

In our proposed liquid lens, the actuation power can be enhanced by increasing the number of LC pistons rather than the operating voltage, therefore, this actuation method is also favorable for large-aperture lens and lens array [23]. Because of the limited electrodes area on the bottom substrate, here we just demonstrate a lens cell in which two liquid lenses

are actuated by four LC pistons. All the dimensions are the same as that of the lens cell shown in Fig. 2(a). As the voltage increases, the optical power of the two lenses is tuned from negative to positive, since the initial diminished images become magnified at $80 V_{\text{rms}}$ as shown in Figs. 3(c)-(d). For easy observation, the aperture holes are circled by red curves. A dynamic switch between the two states is shown in Fig. 3(d) (Media 4). The image changed continuously and uniformly in the transition and no obvious aberration was observed.

Figure 4(a) indicates that there is a threshold of $\sim 40 V_{\text{rms}}$ in the lens actuation. Since the actuation power can be enhanced by increasing the number of LC pistons rather than the operating voltage, it is critically important to reduce the threshold for low-voltage operation. For a single LC piston, the threshold depends on the exerted dielectric force and the interfacial tension along the three-phase contact line (Teflon-LC- L_s), which can be reduced by using narrower-gap stripe electrodes, surrounding liquid with smaller dielectric constant, smaller LC droplet and thinner Teflon layer. If the voltage is too high, crosstalk between two stretched LC droplets (e.g. LC_1 and LC_2 , or LC_3 and LC_4 in Fig. 2(a)) will appear and the actuation power will be severely degraded. In practical applications, the LC droplets should be separated by a black matrix in the chamber. The switching time is affected by the liquid interfacial tension and flow viscosity, and it can be improved by using a surrounding liquid with lower viscosity. Overall speaking, to optimize the device performance, parameters of the lens cell, e.g. the hole size, layout of the holes, cell gap, top slab thickness and electrodes pattern, need to be further studied. To achieve good mechanical stability, a third liquid which is immiscible and has good density match with both ZLI-4389 and silicone oil could be adopted in the lens cell. Its refractive index and surface tension should also be different from that of the silicone oil. Such a liquid helps to minimize the gravity effect and strengthen the liquid-liquid interface confinement at the aperture hole [24]. In our experiments, we use a liquid-air interface as the refractive surface, because it is difficult to find a third liquid which satisfies the above-mentioned criteria in our lab. Since the droplets in the demonstrated lens cell are in millimeter-scale, the lens works well in horizontal placement but gravity effect appears in vertical placement. For the micron-sized droplets, the surface tension dominates over the gravity, thus the microlens should be free from gravity effect even without the third liquid [25]. Meanwhile, lower operating voltage and faster response time are also expected [21]. Microlens array based on this actuation method is promising for parallel processing and sample analysis in lab-on-chip systems.

4. Conclusion

We demonstrate an adaptive liquid lens actuated by LC pistons. The LC droplet with a reciprocating movement functions like a piston, which can effectively tune the lens surface and corresponding optical power. For a 2-mm-aperture lens actuated by four LC pistons, BFD is changed from -5.5 mm to infinity to ~ 66.5 mm as the voltage increases from zero to $80V_{\text{rms}}$. The competitive features are compact size, simple fabrication, good optical performance, lower power consumption (\sim mW) and reasonably fast switching time (\sim 17 ms). Surface treatment and fine processing will help to improve the lens performance and widen the dynamic range. Since the actuation power can be enhanced by increasing the number of LC pistons rather than the operating voltages, it is possible to significantly actuate a large-aperture lens or lens array at a relatively low operating voltage.

Acknowledgments

This work is partially supported by AFOSR under contract No. FA95550-09-1-0170.